JOURNAL OF MODERN SCIENCE
SPECIAL ISSUE
3/57/2024
www.jomswsge.com

DOI: doi.org/10.13166/jms/191406

MICHAŁ GOŁĄBEK
Netrix S.A., Poland
ORCID iD: orcid.org/0000-0002-2696-505X

ZBIGNIEW ORZEŁ
WSEI University in Lublin, Poland
ORCID iD: orcid.org/0000-0002-6356-1695

KONRAD GAUDA
WSEI University in Lublin, Poland
ORCID iD: orcid.org/0000-0002-7300-6978

LESZEK GIL
WSEI University in Lublin, Poland
ORCID iD: orcid.org/0000-0001-8978-7388

ANALYSIS OF ULTRASONIC MEASUREMENT DATA FROM MEDICAL MODELS

ANALIZA DANYCH Z POMIARÓW ULTRADŹWIĘKOWYCH MODELI MEDYCZNYCH

Abstract

This study's primary goal is to improve the accuracy and efficiency of acoustic wave propagation simulations using circular probe models in ultrasonography. This research aims to develop a detailed understanding of how variations in boundary conditions and wave characteristics influence the fidelity of ultrasound imaging. A range of simulation techniques were employed, focusing on non-dispersive and dispersive scenarios, to model acoustic wave behavior comprehensively. The study utilized Gaussian beamforming techniques and improved kernel functions to refine the resolution and decrease computational overhead. Various scenarios were simulated to analyze the impact of wave scattering and dispersion on imaging outcomes. The simulations demonstrated significant improvements in image resolution and accuracy. The refined methods allowed for more apparent distinctions in wave behavior under different boundary conditions, providing deeper insights into wave propagation dynamics. The results confirmed that controlling dispersion and scattering is critical for enhancing imaging quality. This research contributes to the field of ultrasonic imaging by presenting advanced simulation methods that offer more accurate and efficient imaging solutions. The study provides valuable insights into optimizing ultrasonic probes and imaging techniques by focusing on the impact of wave characteristics and boundary conditions. The findings have significant implications for medical diagnostics and material characterization, suggesting potential improvements in ultrasound technology for better patient outcomes and more precise material assessments.

Streszczenie

Głównym celem badań jest poprawa dokładności i wydajności symulacji propagacji fal akustycznych przy użyciu modeli sond kołowych w ultrasonografii. Badania te mają na celu szczegółowe zrozumienie sposobu w jaki zmiany warunki brzegowe i charakterystyki fal wpływają na wierność obrazowania ultrasonograficznego. Zastosowano szereg technik symulacyjnych, koncentrując się na scenariuszach niedyspersyjnych i dyspersyjnych, aby kompleksowo modelować zachowanie fal akustycznych. W badaniu wykorzystano techniki formowania wiązki Gaussa i ulepszone funkcje jądra w celu udoskonalenia rozdzielczości i zmniejszenia obciążenia obliczeniowego. Przeprowadzono symulacje różnych scenariuszy w celu przeanalizowania wpływu rozpraszania fal i dyspersji na wyniki obrazowania. Symulacje wykazały znaczną poprawę rozdzielczości i dokładności obrazu. Udoskonalone metody pozwoliły na wyraźniejsze rozróżnienie zachowania fal w różnych warunkach brzegowych, zapewniając lepszy wgląd w dynamikę propagacji fal. Wyniki potwierdziły, że kontrolowanie dyspersji i rozpraszania ma kluczowe znaczenie dla poprawy jakości

obrazowania. Badania te wnoszą wkład w dziedzinę obrazowania ultradźwiękowego, prezentując zaawansowane metody symulacji, które oferują dokładniejsze i wydajniejsze rozwiązania w zakresie obrazowania. Koncentrując się na wpływie charakterystyki fal i warunków brzegowych, badania wnoszą wkład w optymalizację sond ultradźwiękowych i technik obrazowania. Uzyskane rezultaty mają znaczący wpływ na diagnostykę medyczną i charakterystykę materiałów, wskazując na potencjalne ulepszenia technologii ultradźwiękowej w celu uzyskania lepszych wyników badania pacjentów i bardziej precyzyjnych analiz zdjęć UST.

Keywords: *Acoustic Wave Propagation, Ultrasound Tomography, Simulation Techniques, Wave Scattering and Dispersion, Beamforming*

Słowa kluczowe: *Propagacja fal akustycznych, tomografia ultradźwiękowa, techniki symulacyjne, rozpraszanie i dyspersja fal, kształtowanie wiązki*

Introduction

This article aims to present the concept and optimization of a tomographic system for ultrasonography (von Ramm et al., 1978). The presented UST device, called UST4, was designed to improve data communication between the measurement cards and the main module and should enable the implementation of an improved measurement method called beamforming. (Kozlowski et al., 2019). Specific research and development goals include several activities. The first is to develop faster communication, which provides for creating a system with separate SPI (Serial Peripheral Interface) communication buses coming out of the FPGA (Field-Programmable Gate Array) for each measurement card. This would allow faster and more efficient data transfers (Shan et al., 2019). As part of this, it is envisioned to synchronously collect data from the measurement cards and transfer it to external RAM, and then to the STM32 microcontroller and transfer it to a PC via USB 2.0 (Rahman et al., 2013).

Another area is work on beamforming. Beamforming is an advanced signal processing technique that alters the phase and amplitude of signals emitted from antennas to generate a directional wavefront. This technique originated in the early 20th century and has developed substantially since its initial use in military sonar systems. The primary distinction between beamforming and conventional ultrasound transducer (UST) systems resides in beamforming's capacity to concentrate energy in precise directions, enhancing signal

quality and diminishing interference (Shan et al., 2019). Contrary to UST, which generally produces sound waves in a broad pattern, beamforming can focus on a specific area with enhanced accuracy (Koulountzios et al., 2019; Nordin et al., 2014). There are numerous benefits to beamforming. Tightly controlling and directing signals enables a more efficient spectrum utilization by reducing the likelihood of signal interference (Cuadra et al., 2005; Liu et al., 2022). This emphasis on directionality also enhances signal-to-noise ratios, a critical factor in environments with much clutter or noise. Beamforming in wireless communications can significantly improve network performance by precisely directing signals toward intended receivers and avoiding unintended ones. This optimization of bandwidth usage and enhancement of overall system capacity are the key benefits of beamforming.

The potential of beamforming extends significantly beyond its current applications. 5G technology is expected to rely heavily on beamforming to handle the significant surge in data traffic and the widespread use of Internet of Things (IoT) devices (Chen et al., 2019; Rymarczyk, Cieplak, et al., 2019). Furthermore, it is expected to play a crucial role in the advancement of emerging technologies, such as self-driving cars, where the capability to transmit and receive signals with great accuracy is of utmost importance (Kłosowski, 2010; Kłosowski et al., 2018). Beamforming in the medical field can enhance imaging techniques, resulting in improved clarity and detail of images used for diagnostic purposes (Qiu et al., 2021). Furthermore, the ability of beamforming to adjust to various frequencies and environments renders it a highly versatile tool (Ning et al., 2023).

The achievement was attained by simulating transmitters and acquiring the wave's directionality. Another notable area of focus was the execution of machine-learning strategies. (Gomes et al., 2020; Rymarczyk, Kozłowski, et al., 2019). Supervised learning techniques used a simulator to solve a direct and inverse problem. This facilitated the utilization of machine learning and deep learning algorithms for the specific objective of analyzing ultrasound data (Oh et al., 2020; Shan et al., 2019). Finally, but certainly not least, one of the most critical aspects of the work was the optimization of parameters. The main goal was to choose parameters and carry out signal conditioning to improve the quality of simulations and better replicate real-world conditions. The scripts underwent refactoring, resulting in the creation of modules. The objective of this project was

to improve the current ultrasound tomography (UST) technology by introducing a new system as well as exploring and utilizing the latest techniques in simulation and data processing (Kłosowski et al., 2020). These activities collectively contributed to the development of a comprehensive project. The advancements in these fields directly improved the quality and efficiency of medical ultrasound imaging, as well as opened up possibilities for new diagnostic applications (Kang et al., 2016; Liang et al., 2021; Tutschek et al., 2017; Yan et al., 2017).

Research Methodology

The research methodology focused on developing the UST4, a next-generation ultrasonographic computer tomography system. The main goals of the research were to improve communication between measurement cards and the main module and incorporate sophisticated beamforming techniques. At first, the idea for the novel design involved using separate SPI communication buses that come from an FPGA for each measurement card. This approach was postulated to facilitate expedited and more streamlined data transfer. Afterward, a preliminary test program for STM32G4 and FPGA was partially developed. A test configuration was assembled to validate the concept, consisting of a pre-existing board containing STM32H7 and FPGA and two NUCLEO boards equipped with STM32G4 that emulated the measurement cards. The data collected simultaneously from all measurement cards was planned to be transferred to an external RAM, then forwarded through an FMC to the STM32, and ultimately transmitted to a PC via USB 2.0. Early endeavors to establish communication with external RAM via FPGA yielded varied results, as specific data could not be retrieved following the writing process. The research involved constructing and evaluating a measurement card consisting of a MAX2082 array and an Altera Cyclone IV FPGA for beamforming. Additionally, a control board with an STM32H7 microcontroller and a set of converters capable of generating various voltages, including high voltages of +/-72V, was used.

Figure 1 on the left shows the measurement board with the MAX2082 chip and BGA-mounted FPGA, while on the right is the board with the STM32H7 with power converters to capture data from the FPGA and transfer it via USB to a PC.

Figure 1. *Assembled beamforming test boards without FPC sockets and tapes*

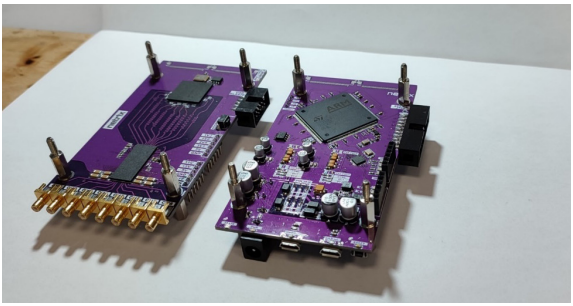

Although the previous UST3 system faced similar problems, such as unstable signals and misaligned components, these issues were resolved by redesigning and optimizing the board to minimize electromagnetic interference. Furthermore, efforts were made to develop novel FPGA blocks that facilitate the reading and writing of the MAX2082's configuration through a bidirectional single-line SPI bus. Upon initializing the FPGA, the measurement system's configuration was loaded and validated by re-reading. This was indicated by the green LED illumination, which signified readiness. In the event of errors, the LEDs would alternate between red (indicating failure), yellow (indicating sleep mode), and blue (indicating a reconfiguration attempt). Research efforts also focused on the challenges of retrieving data from the measurement system's ADC converters. Despite undergoing a thorough redesign and optimization to minimize electromagnetic interference, the FPGA still needed help with unreadable signals despite appearing acceptable when observed on an oscilloscope. As a result, a distinct power module was developed, incorporating low-drop stabilizers to eliminate any impact from the power supply effectively. During the research, there was a persistent cycle of testing, identifying problems, and implementing solutions. The iterative process played a crucial role in accomplishing the objectives of the UST4 development, which aimed to improve the efficiency and effectiveness of ultrasonographic imaging.

Boundary Problem Solutions and Wave Propagation Simulations

In previous research, substantial progress was achieved in developing scripts for simulating the propagation of sound waves. An innovative resolution to the issue of the *free-space* boundary problem was suggested, signifying a significant change in the methodology of acoustic simulations. This innovative approach facilitated a substantial decrease in memory consumption, optimizing it from a quadratic time complexity of to a linear time complexity of . This optimization not only improved the technical aspects but also enabled a more sophisticated simulation of wave scattering. By modifying simulation methods, it has become feasible to manipulate the duration of noise reduction within the tomographic probe, as well as the ability of the wave to penetrate, thereby improving the precision and effectiveness of the simulations. These technological advancements have established a solid basis for studying wave dynamics in uncontrolled environments, essential for applications that demand accurate imaging and diagnostics. The capacity to replicate wave propagation without artificial boundaries or reflections resulted in more accurate models and results. The enhancement in memory efficiency accelerated and expanded the simulations and enabled the modeling of more intricate scenarios without a substantial augmentation in computational resources.

In the study, a script was developed to simulate the propagation of acoustic waves using a circular probe model with uniformly distributed sensors along its circumference. This model was the foundation for investigating various boundary conditions and their implications for wave behavior within the simulated domain. Initially, matrix boundary conditions were implemented to account for the acoustic impedance of the *walls* surrounding the simulated area. Using numerical experiments showed that adding dissipative boundary conditions did not entirely stop waves from traveling across the simulation domain's edges.

Mathematical Analysis of the Model

The need to increase the simulation area about the FoV (Field of View) causes more pixels to be reconstructed than results from the size of the FoV itself. Using a simulation implementation based on the matrix equation, we have:

$$u^{t+1} = (\lambda B + I)^{-1}(2I + \lambda^2 L)\, u^t + (\lambda B - I)\, u^{t-1} \tag{1}$$

We, therefore need to store two matrices of size , where the simulation is performed on the area of size $n \times n$.

The rigid implementation of Dirichlet conditions simplifies the equation step to the formula:

$$u^{t+1} = (2I + \lambda^2 L)\, u^t - u^{t-1} \tag{2}$$

which still needs at least one matrix of size $n^2 \times n^2$, that means that the simulation still needs memory of the order of $0(n^2)$.

To reduce this problem, we used an equivalent implementation, based on a convolutional filter:

$$u^{t+1} = 2u - u^{t-1} + \lambda^2 Conv(u, L) \tag{3}$$

where:

$$L = \begin{pmatrix} 0 & 1 & 0 \\ 1 & -4 & 1 \\ 0 & 1 & 0 \end{pmatrix}$$

represents a filter that implements discrete Laplacian. As a result, apart from the need to store the arrays u^{t+1}, u^t, u^{t-1} u in memory, there is no need for additional memory beyond the 3×3 array of the convolutional filter. Also note that such an implementation does not require the expansion of matrices into vectors, as in the case of matrix equations.

In addition, through experimentation, it seems that the simulation is more stable for the *soft* variant of Laplacian:

$$L^* = \begin{pmatrix} 0.25 & 0.5 & 0.25 \\ 0.5 & -3 & 0.5 \\ 0.25 & 0.5 & 0.25 \end{pmatrix} \tag{4}$$

which is currently used in the simulation. The condition for the stability of the simulation for the Laplacian *L* is the so-called Courant-Friedrichs-Lewy condition:

$$\lambda = \frac{v\ dt}{dx} \leq \sqrt{0.5} \approx 0{,}0707. \tag{5}$$

where:
v – the wave speed at the node, d x – the distance between the nodes, dt – the n-th of the time step. In practice, in this condition, we select the values *dt* and *dx* in such a way that:

$$\lambda_c = \frac{c\ dt}{dx} = 0{,}07, \tag{6}$$

where *c* is the maximum wave velocity used in the simulation.

Figure 2. *Passing a wave through an obstacle (86th frame of the simulation) that does not satisfy, theoretically, the CFL condition* ($lam=1.2 \cdot \lambda_c$)*, using: (a) – Laplacian L (with destabilization artifact) and (b) – Laplacian L* (without destabilization artifact)*

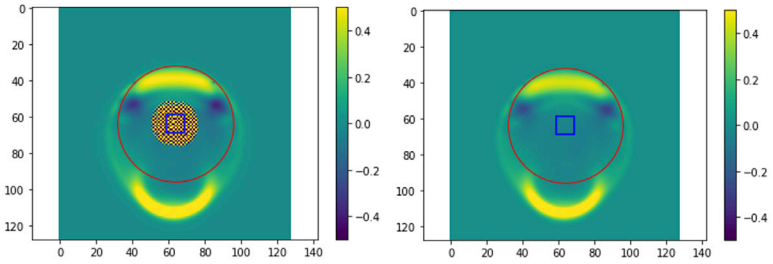

An additional aspect of the simulation is that during the measurement series, we have to wait after stimulating one sensor until the acoustic wave in the interior is attenuated so that it does not interfere with the wave generated by the next transmitter. In the current scheme, the scattering factor was not considered, meaning the probe's interior never reached complete silence. To control the wave's scattering, we added a filter with a Gaussian nucleus to the simulation step. In this way, by controlling the filter's variance, the wave's scattering can be increased.

Simulation research

The simulations were conducted utilizing a computational grid composed of 128×128 spatial nodes, running for a total of 8000 steps. These simulations modeled the dynamics within a 40×40 cm square area and featured a circular probe with a 20 cm diameter. The temporal structure of the simulation involved the sequential activation of 16 sensors. Each sensor was excited at 500-step intervals for a duration of 20 iterations, employing a sinusoidal excitation function defined as $U=A\sin(\omega t)$, where stood for amplitude, set at a value of 10, and represented the angular frequency, set at 1.0. The complete sequence of the simulation, encompassing 8000 iterations for all 16 sensors, was computed in approximately 7 seconds using an i9-11900F processor. Considering the stability conditions of the simulation, this computational time translated to less than 12 milliseconds of real-time probe operation. This level of efficiency in simulation performance indicated the potential for these computational models to be used in real-time applications despite the complexity of the simulated probe's environment.

Figure 3 depicts the 390th frame of the simulation, demonstrating the propagation of the acoustic wave within the tomographic probe without any dispersion . This visual representation captures the dynamics of the sound wave as it interacts with the environment under nondispersive conditions. The absence of dispersion means the wave maintains high coherence and exhibits minimal spreading as it travels through the medium. In this frame, the wavefronts appear well-defined and sharp, illustrating the effect of a perfectly elastic medium in which the wave does not lose energy due to scattering or absorption.

Figure 3. *View of the 390th simulation frame without scattering (σ=0)*

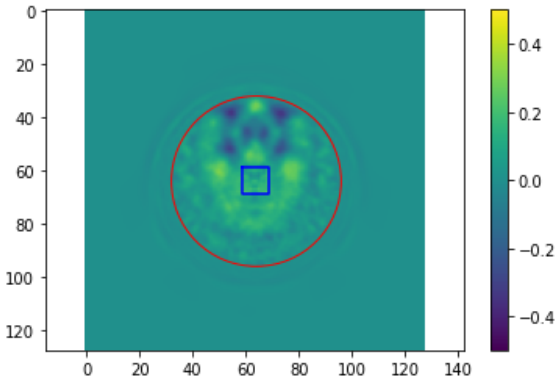

This condition is idealized in computational simulations to study the intrinsic properties of the wave and the medium's response without the complexity introduced by wave dispersion. For this scenario, the simulation settings did not include the Gaussian kernel, which would typically introduce dispersion and simulate more realistic physical interactions such as molecular diffusion or medium heterogeneity. As a result, the simulation provides a clear picture of the wave's behavior in a controlled environment, which is critical for understanding fundamental wave dynamics and calibrating the simulation settings before introducing more complex boundary conditions or dispersion effects. This frame serves as a baseline for comparing the impact of different dispersion coefficients on wave propagation, and it can be beneficial for theoretical explorations of wave mechanics in free-space or minimally obstructive environments. The wave pattern is obvious and simple when , which is very different from situations where parameters change the wave's transmission. This shows how much the properties of the medium affect how acoustic waves travel. This allows us to control the time needed to silence the wave inside the probe. Figure 4 depicts the 390th frame of the same simulation as Figure 3, but with the inclusion of dispersion, represented by a dispersion coefficient (σ=0.4). This visualization contrasts the non-dispersive scenario in Figure 3, where the wave maintained sharp, well-defined frontiers as it propagated through the medium. In Figure 4, introducing the dispersion coefficient fundamentally alters the wave's appearance and behavior. The wavefronts in this frame are noticeably more diffuse and spread out, lacking the sharpness observed in the nondispersive case. This effect is due to the Gaussian kernel applied in the simulation, which models the physical phenomena of energy dispersion and wave scattering within the medium.

The dispersion results in a smoothing of the wave's energy over a broader area, reducing the peak intensity but increasing the coverage area of the acoustic signal. This is a critical aspect for applications such as medical imaging or materials testing, where the ability to control and understand the scattering of waves can significantly impact the accuracy and resolution of the imaging results.

Figure 4. *View of the 390th simulation frame with the same parameters but with a spread (σ=0.4)*

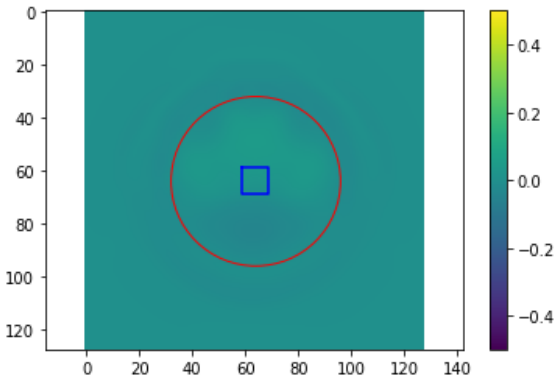

Comparing Figures 5 and 6 highlights the significant impact of dispersion on wave propagation. The non-dispersive model (Figure 5) shows how waves move clearly and are idealized. The dispersive model (Figure 6) makes the simulation more realistic and shows how the properties of the medium and how waves interact with it can affect how acoustic technologies are used in real life. This comparison helps to understand the physical properties of waves but also helps to refine simulation parameters for more accurate modeling of real-world scenarios. By considering the scattering, we can obtain much cleaner measurement waveforms because the calming of the wave does not interfere with the measurement read in the vicinity of the sensors. The first extreme will be the variant without attenuation, with significant wave collimation and lack of muting. These two pictures, Figure 8 (called *Measurement of probe No. 0 for the first 2000 steps of the simulation at (σ=0)* and Figure 9 (called *Wave collimation effect on the circular edge of the probe (σ=0)*, show how a non-dispersive setting (σ=0) changes the behavior and measurement of sound waves in a controlled simulation environment. Figure 5 shows the data collected from probe number 0 during the initial 2000 simulation steps, where no dispersion (σ=0) is applied. In this scenario, the acoustic wave is depicted as maintaining high coherence and intensity throughout the propagation process.

Figure 5. *Measurement of probe No. 0 for the first 2000 simulation steps at σ=0*

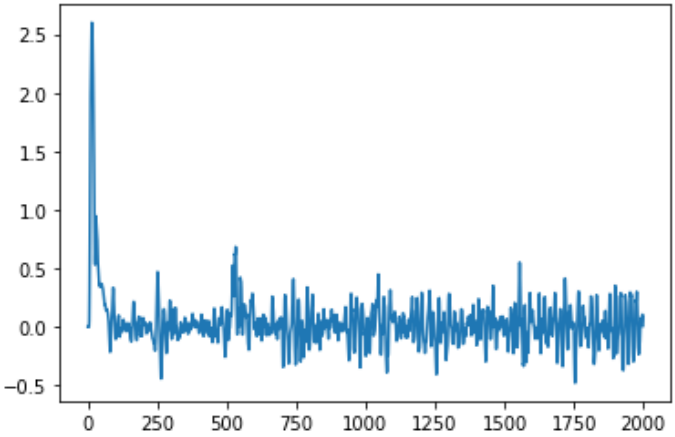

The simulation under these parameters allows the wave to travel without scattering, maintaining its original energy distribution and directionality. This condition is particularly useful for analyzing the probe's sensitivity and undisturbed behavior, providing a baseline measurement of the acoustic wave's propagation in a perfectly elastic medium. Figure 6 depicts the effect of wave collimation at the circular edge of the probe, again under nondispersive conditions . Collimation refers to the process by which wave fronts become more parallel and focused, resulting in minimal spread as the wave exits the probe. This effect is critical in applications that require precise wave directionality, such as focused ultrasound therapies or certain imaging techniques.

The visual representation in Figure 6 highlights how the wave retains a narrow shape and directional integrity when interacting with the probe's circular boundary, emphasizing the probe's role in shaping the wave's path and focusing its energy. Both figures demonstrate the characteristics of wave propagation without dispersion. The high coherence and focus observed in these simulations indicate the waves' potential for applications requiring precise energy delivery and minimal energy loss over distance.

Figure 6. *Wave collimation effect on the circular edge of the probe (σ=0)*

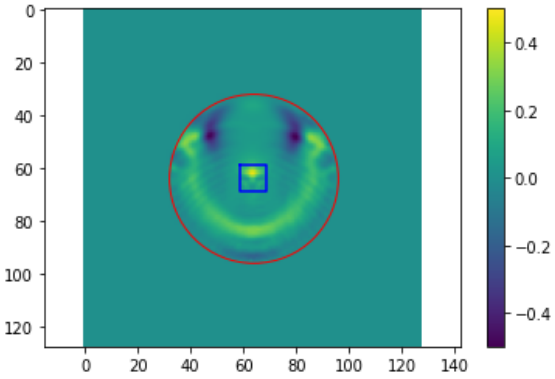

However, they also emphasize the importance of considering dispersion in real-world applications, where environmental and material properties can significantly alter these ideal behaviors. These visual data points provide a foundational comparison for understanding how dispersion and other factors influence acoustic wave dynamics in more complex scenarios. On the other hand, too high attenuation results in an almost undisturbed passage of the wave through the probe, eliminating the collimation effect.

Figure 7. *Significant 'blurring' (waves) canceling out collimation σ=1.0)*

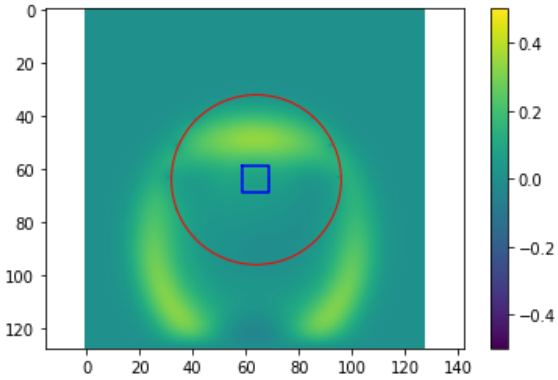

On the other hand, we get much *cleaner* impulse waveforms visible in Figure 8. Ultimately, the values allow for a consensus between the two phenomena. The selection of this parameter will have to be verified with a real UST scanner.

Figures 5 and 6 depict a simulation environment with a dispersion coefficient (σ) set to 0, signifying no dispersion. Figure 5 shows the waveform from probe No. 0 over the first 2000 steps, maintaining sharp features and high amplitude throughout, indicating minimal energy loss or distortion. This suggests that highly coherent wave propagation is unaffected by the medium.

Figure 8. *Measurement of probe No. 0 for the first 2000 simulation steps at σ=1.0*

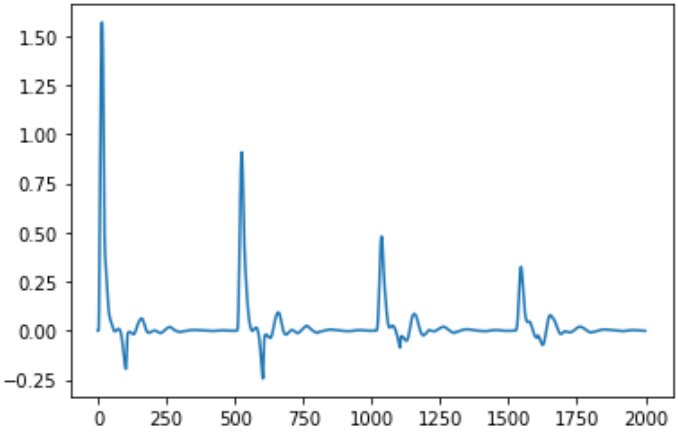

Figure 6 demonstrates the collimation effect at the probe's circular edge under non-dispersive conditions (σ = 0). The wave remains focused and narrow, emphasizing efficient wave direction without scattering, which is ideal for precise directional wave energy control.

In contrast, Figures 7 and 8 illustrate simulation conditions with a higher dispersion coefficient (σ = 1.0), resulting in significant changes in wave behavior. Figure 7 displays a blurring effect, with the waveform spreading across the medium and losing its focused path. This indicates much energy dispersion, similar to heterogeneous materials or absorbing energy. In high-dispersive conditions, Figure 8 shows measurement data from probe No. 0. It is very different from Figure 5, with less amplitude and a longer, more spread-out

waveform that doesn't have sharp peaks and troughs. This indicates significant diffusion of acoustic energy, leading to less precise but more broadly distributed wave impacts.

Analyzing Figures 5–8, some key differences can be distinguished. The wave maintains sharp, well-defined features in the non-dispersive setting ($\sigma = 0$). The waveform is significantly smoothed and broadened in dispersive ($\sigma = 1.0$). Considering energy distribution, non-dispersive models concentrate energy efficiently, making them suitable for precise interventions or imaging. Dispersive models spread energy over a wider area, beneficial for broader impacts, such as certain non-invasive therapies or imaging techniques.

Regarding application implications, non-dispersive models are critical for scenarios requiring precision and control over wave propagation. Dispersive models provide insights into wave behavior in complex media, offering a more realistic depiction of scenarios involving heterogeneous materials.

Conclusions

This study makes big steps forward in simulating how acoustic waves travel using a circular probe model. It shows how wave behavior and boundary conditions interact in complex ways. The findings underscore the importance of considering non-dispersive and dispersive settings to model wave dynamics in medical and material testing applications accurately. The research shows that using better simulation methods, such as Gaussian kernels and beamforming strategies, makes ultrasound imaging simulations much more accurate and believable. The novel methodologies have shown that precise control over wave dispersion and scattering can drastically affect the accuracy and resolution of imaging outcomes. This is particularly relevant in fields requiring high-resolution images, such as medical diagnostics and material characterization. Furthermore, the study's approach to reducing computational demands through optimized simulation algorithms contributes significantly to the feasibility of more complex and realistic modeling scenarios. The implications of this research extend beyond theoretical modeling, offering practical insights into the design

and optimization of ultrasonic imaging systems. The advancements in simulation technology described herein not only improve our understanding of acoustic wave behavior but also pave the way for future innovations in ultrasonic imaging technology. These contributions are poised to substantially impact the development of next-generation diagnostic tools, potentially leading to improved patient outcomes and more precise material testing. Overall, this research provides a comprehensive foundation for further exploration and development within the field of acoustic wave simulations, suggesting numerous avenues for future studies to build upon the methodologies and findings discussed.

References

Chen, X., Tang, S., Lu, Z., Wu, J., Duan, Y., Huang, S. C., & Tang, Q. (2019). IDiSC: A New Approach to IoT-Data-Intensive Service Components Deployment in Edge-Cloud-Hybrid System. *IEEE Access*, *7*, 59172–59184. https://doi.org/10.1109/ACCESS.2019.2915020

Cuadra, M. B., Cammoun, L., Butz, T., Cuisenaire, O., & Thiran, J. P. (2005). Comparison and validation of tissue modelization and statistical classification methods in T1-weighted MR brain images. *IEEE Transactions on Medical Imaging*, *24*(12). https://doi.org/10.1109/TMI.2005.857652

Gomes, J. C., Barbosa, V. A. F., Ribeiro, D. E., de Souza, R. E., & dos Santos, W. P. (2020). Electrical impedance tomography image reconstruction based on backprojection and extreme learning machines. *Research on Biomedical Engineering*, *36*(4), 399–410. https://doi.org/10.1007/S42600-020-00079-3

Kang, L., Zhang, C., Chen, P., Li, J., & Zhang, Y. (2016). Electromagnetic ultrasonic tomography of plate defects based on omnidirectional Lamb-wave EMATs. *Proceedings of 2015 IEEE Far East NDT New Technology and Application Forum, FENDT 2015*. https://doi.org/10.1109/FENDT.2015.7398313

Kłosowski, G. (2010). Design for a hybrid single multi-load AGV simulation system with artifficial intelligence controller. *Applied Computer Science*, *6*(2), 81–94.

Kłosowski, G., Gola, A., & Amila, T. (2018). Computational Intelligence in Control of AGV Multimodal Systems. *IFAC-PapersOnLine*, *51*(11), 1421–1427. https://doi.org/10.1016/j.ifacol.2018.08.315

Kłosowski, G., Rymarczyk, T., Cieplak, T., Niderla, K., & Skowron, Ł. (2020). Quality assessment of the neural algorithms on the example of EIT-UST hybrid tomography. *Sensors (Switzerland)*, *20*(11). https://doi.org/10.3390/s20113324

Koulountzios, P., Rymarczyk, T., & Soleimani, M. (2019). A Quantitative Ultrasonic Travel-Time Tomography to Investigate Liquid Elaborations in Industrial Processes. *Sensors*, *19*(23), 5117. https://doi.org/10.3390/s19235117

Kozlowski, E., Rymarczyk, T., & Klosowski, G. (2019). Logistic regression application to image reconstruction in UST. *2019 Applications of Electromagnetics in Modern Engineering and Medicine, PTZE 2019*. https://doi.org/10.23919/PTZE.2019.8781722

Liang, G., Dong, F., Kolehmainen, V., Vauhkonen, M., & Ren, S. (2021). Nonstationary Image Reconstruction in Ultrasonic Transmission Tomography Using Kalman Filter and Dimension Reduction. *IEEE Transactions on Instrumentation and Measurement*, *70*. https://doi.org/10.1109/TIM.2020.3031172

Liu, X., Zhang, T., Ye, J., Tian, X., Zhang, W., Yang, B., Dai, M., Xu, C., & Fu, F. (2022). Fast Iterative Shrinkage-Thresholding Algorithm with Continuation for Brain Injury Monitoring Imaging Based on Electrical Impedance Tomography. *Sensors 2022, Vol. 22, Page 9934*, *22*(24), 9934. https://doi.org/10.3390/S22249934

Ning, B., Tian, Z., Mei, W., Chen, Z., Han, C., Li, S., Yuan, J., & Zhang, R. (2023). Beamforming Technologies for Ultra-Massive MIMO in Terahertz Communications. *IEEE Open Journal of the Communications Society*, *4*. https://doi.org/10.1109/OJCOMS.2023.3245669

Nordin, N., Idroas, M., Zakaria, Z., & Ibrahim, M. N. (2014). Tomographic image reconstruction of monitoring flaws on gas pipeline based on reverse ultrasonic tomography. *2014 5th International Conference on Intelligent and Advanced Systems (ICIAS)*, 1–6. https://doi.org/10.1109/ICIAS.2014.6869445

Oh, S., Kim, H. K., Jeong, T.-E., Kam, D.-H., & Ki, H. (2020). Deep-Learning-Based Predictive Architectures for Self-Piercing Riveting Process. *IEEE Access*, *8*, 116254–116267. https://doi.org/10.1109/ACCESS.2020.3004337

Qiu, W., Bouakaz, A., Konofagou, E. E., & Zheng, H. (2021). Ultrasound for the Brain: A Review of Physical and Engineering Principles, and Clinical Applications. *IEEE Transactions on Ultrasonics, Ferroelectrics, and Frequency Control*, *68*(1). https://doi.org/10.1109/TUFFC.2020.3019932

Rahman, F., Yunus, M., Azida, N., Azlan, N., Muhammad, J., Pusppanathan, F., Jumaah, C. L., Goh, A., Rahim, A., Ahmad, Y., Md, Y., & Rahim, H. A. (2013). Simulation Study of Bubble Detection Using Dual-Mode Electrical Resistance and Ultrasonic Transmission Tomography for Two-Phase Liquid and Gas. In *Sensors & Transducers* (Vol. 150). http://www.sensorsportal.com

Rymarczyk, T., Cieplak, T., Klosowski, G., & Kozlowski, E. (2019). Monitoring the natural environment with the use of IoT based system. *2019 Applications of Electromagnetics in Modern Engineering and Medicine, PTZE 2019*. https://doi.org/10.23919/PTZE.2019.8781746

Rymarczyk, T., Kozłowski, E., Kłosowski, G., & Niderla, K. (2019). Logistic Regression for Machine Learning in Process Tomography. *Sensors 2019, Vol. 19, Page 3400*, *19*(15), 3400. https://doi.org/10.3390/S19153400

Shan, H., Wiedeman, C., Wang, G., & Yang, Y. (2019). *Simultaneous reconstruction of the initial pressure and sound speed in photoacoustic tomography using a deep-learning approach*. 4. https://doi.org/10.1117/12.2529984

Tutschek, B., Braun, T., Chantraine, F., & Henrich, W. (2017). Computed tomography and ultrasound to determine fetal head station. *Ultrasound in Obstetrics & Gynecology*, *49*(2), 279–280. https://doi.org/10.1002/UOG.17291

von Ramm, O. T., Smith, S. W., & Kisslo, J. A. (1978). Ultrasound Tomography of the Adult Brain. *Ultrasound in Medicine*, 261–267. https://doi.org/10.1007/978-1-4613-4021-8_73

Yan, B., Wu, C., & Ma, H. (2017). Study on the method of nonmetallic defects based on ultrasonic tomography and morphology. *2017 12th IEEE Conference on Industrial Electronics and Applications (ICIEA)*, 1287–1292. https://doi.org/10.1109/ICIEA.2017.8283037